
Fractional energy states of strongly-interacting bosons in one dimension

N. T. ZINNER¹, A. G. VOLOSNIIEV¹, D. V. FEDOROV¹, A. S. JENSEN¹ and M. VALIENTE²

¹ *Department of Physics and Astronomy, Aarhus University, DK-8000 Aarhus C, Denmark*

² *SUPA, Institute for Photonics and Quantum Sciences, Heriot-Watt University, Edinburgh EH14 4AS, United Kingdom*

PACS 03.65.Ge – Solutions of wave equations: bound states

PACS 03.75.Hh – Static properties of condensates; thermodynamical, statistical, and structural properties

PACS 67.85.Fg – Multicomponent condensates; spinor condensates

Abstract – We study two-component bosonic systems with strong inter-species and vanishing intra-species interactions. A new class of exact eigenstates is found with energies that are *not* sums of the single-particle energies with wave functions that have the characteristic feature that they vanish over extended regions of coordinate space. This is demonstrated in an analytically solvable model for three equal mass particles, two of which are identical bosons, which is exact in the strongly-interacting limit. We numerically verify our results by presenting the first application of the stochastic variational method to this kind of system. We also demonstrate that the limit where both inter- and intra-component interactions become strong must be treated with extreme care as these limits do not commute. Moreover, we argue that such states are generic also for general multi-component systems with more than three particles. The states can be probed using the same techniques that have recently been used for fermionic few-body systems in quasi-1D.

Introduction. – Ultracold atomic gas experiments have proven an invaluable tool for realizing strongly-correlated quantum mechanical systems in highly tunable environments [1]. A prominent example is the so-called Tonks-Girardeau (TG) gas [2, 3] of impenetrable bosons in one dimension (1D) that has been created using cold atoms [4–7]. An exciting recent advance in this direction is the ability to produce and manipulate low-dimensional samples with controllable particle numbers down to single digits [8–12]. These developments show that few-body systems with bosons and fermions in microtraps that can be manipulated and studied in great detail can be achieved with ultracold atoms. These systems would facilitate access to strongly correlated states with applications in quantum information, computation, and atomtronics [13–19].

One-dimensional quantum systems have served as playgrounds for many theorists due to the presence of exact solutions. Most of these are built on the Bethe ansatz first introduced for studying magnetism in 1D metals [20]. The new possibilities for trapping cold atoms with tunable short-range interactions in effective 1D geometries

has generated frenetic recent activity [21–28]. While many of these works use different generalizations of the original Bose-Fermi mapping of Girardeau [3], it was recently shown that the mapping fails for the case of trapped two-component Fermi gases already at the few-body level [29–33], ushering in the need for a more general technique to address multi-component fermionic systems [34]. This begs the question of whether there could be some overlooked features of two-component Bose systems in the strongly-interacting regime. A recent numerical study [28], suggests that there is a non-trivial crossover between the composite fermionized regime (weak intra-component and strong inter-component interactions [22]) and a regime of phase separation when one of the components attains strong inter-component repulsion.

In this paper we describe a class of states for two-component bosons with strong short-range interactions that is different from those obtained by a Bose-Fermi mapping to spinless fermions [3]. We demonstrate this using a model for three harmonically trapped equal mass particles where two are identical bosons of type *A* and the third of a distinct type, *B*. When the *A* bosons are non-interacting,

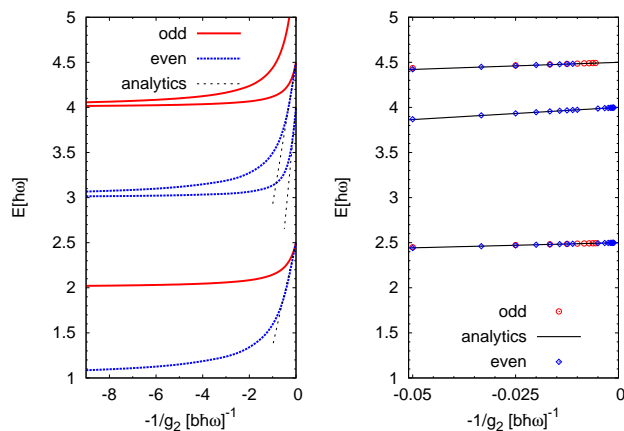


Fig. 1: Energy spectra obtained using the stochastic variational method. Left panel shows the energy on for repulsive $g_2 > 0$ interactions for the lowest even and odd states in the spectrum. The right panel shows a zoom of the same data around $g_2^{-1} = 0$ and includes analytical results for the energy to first order in g_2^{-1} . We clearly see the analytical and numerical results merge close to resonance, proving the convergence of our calculations.

we find two types of eigenstates when the AB interaction becomes strong; one set can be related to the wave function of spinless fermions whereas the others (including the ground state) have wave functions that are highly correlated and cannot be obtained or built by a mapping to fermions. This could be regarded as natural when one species is non-interacting. However, we show that even in this case a subset of the spectrum can in fact be obtained by a Bose-Fermi mapping. In sharp contrast to states related to spinless fermions, the new class of states will generally have energy eigenvalues that are not integer multiples of the harmonic oscillator energy unit (disregarding zero-point energies). We confirm the analytical finding by a stochastic variational calculation which is, to the best of our knowledge, the first time this technique has been applied to strongly-interacting one-dimensional systems. Furthermore, we show that the limit where both AA and AB interactions become strong is very delicate and yields different eigenstates depending on the order in which the couplings are taken to infinity. As we demonstrate below, our findings imply that general multi-component N -boson systems will have such solutions and they must be considered when addressing strongly-interacting 1D bosonic systems. We also show that current experimental techniques using either tunneling out of a trap or RF spectroscopy should be able to see a clear distinction between the integer and fractional energy states in these strongly-interacting systems.

Model. – We consider two identical bosons (A) with coordinates x_1 and x_2 and a third particle (B) with coordinate x_3 which is distinct from the bosons but of the same mass, m . This can be realized using bosons with two different internal (hyperfine) states in the context of

cold atoms [1]. The particles move in a harmonic oscillator with frequency ω and oscillator length $b = \sqrt{\hbar/m\omega}$ and have short-range pair potentials that we model as delta functions, i.e.

$$V = g_1\delta(x_1 - x_2) + g_2\delta(x_1 - x_3) + g_2\delta(x_2 - x_3). \quad (1)$$

Defining the coordinates $x = (x_1 - x_2)/\sqrt{2}$, $y = (x_1 + x_2)/\sqrt{6} - \sqrt{2/3}x_3$, and $R = (x_1 + x_2 + x_3)/\sqrt{3}$, we may separate the center-of-mass, R , and consider the relative wave function, $\Psi(x, y)$. Bosonic symmetry requires $\Psi(-x, y) = \Psi(x, y)$ and since our system is parity invariant, the parity is thus determined by the sign of $\Psi(x, y)$ when $y \rightarrow -y$. This means that once we have the solution for $x > 0$ and $y > 0$, the full solution can be obtained by continuation using parity and Bose symmetry. Away from the points at which two particles meet, the solutions must be eigenfunctions of the free Hamiltonian for three particles in a harmonic trap. The two regular normalizable solutions are [35]

$$\Psi(\rho, \phi) = N\rho^\mu U(-\nu, \mu + 1, \rho^2) e^{-\rho^2/2} \begin{cases} \cos(\mu\phi) \\ \sin(\mu\phi) \end{cases}, \quad (2)$$

where $U(a, b, x)$ is the Tricomi function, $\rho = \sqrt{x^2 + y^2}$ is the hyperradius, $\phi = \arctan(y/x)$ the hyperangle, and N is a normalization constant. The corresponding energy is $E = \hbar\omega(2\nu + \mu + 1)$.

The interactions can be implemented by matching solutions in different regions of space through continuity of the wave function and the conditions

$$\frac{\hbar^2}{2m\rho^2} \left(\frac{d\Psi(\rho, \phi)}{d\phi} \Big|_{\phi_0+\epsilon} - \frac{d\Psi(\rho, \phi)}{d\phi} \Big|_{\phi_0-\epsilon} \right) = \frac{g_i}{\sqrt{2}\rho} \Psi(\rho, \phi_0), \quad (3)$$

for any ρ and where ϕ_0 is an angle where two particles overlap ($i = 1$ for AA overlap and $i = 2$ for AB overlap). We now define rescaled coupling strengths, $\tilde{g}_i = \sqrt{2}m\rho g_i/\hbar^2$. In terms of the \tilde{g}_i , Eq. (3) is now independent of ρ and we have achieved an effective decoupling of the radial and angular equations. The decoupling means that we get an equation that is independent of ν . The crucial point is that when either $g_1 \rightarrow \infty$ and $g_2 = 0$, $g_2 \rightarrow \infty$ and $g_1 = 0$, or $g_1 = g_2 \rightarrow \infty$, our model is exact. Our model can thus be used to obtain the exact wave functions and energies in limits where one or both couplings are large.

The even parity solutions can be obtained by assuming that the angular wave function, $F_i(\phi)$, has the form, $F_1(\phi) = \alpha \cos(\mu\phi)$, an even function in ϕ and thus in $y \rightarrow -y$, for $0 < \phi < \pi/6$. In the region $\pi/6 < \phi < \pi/2$, we assume the general form $F_2(\phi) = \beta \sin(\mu\phi + \delta)$. α , β , and δ are constants. Using continuity and Eq. (3) at $\phi_0 = \pi/6$ and $\phi_0 = \pi/2$ gives the eigenvalue equation that determines μ ,

$$-\mu \cot\left(\frac{\pi}{3}\mu + \arctan\left(\frac{2\mu}{\tilde{g}_1}\right)\right) + \mu \tan\left(\frac{\pi}{6}\mu\right) - \tilde{g}_2 = 0. \quad (4)$$

When $g_1 = 0$ and $g_2 \rightarrow \infty$ our model is exact and we have thus obtained a whole class of solutions indexed by ν .

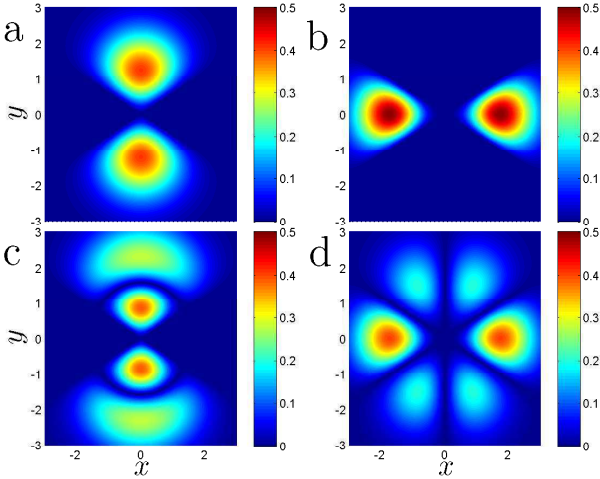


Fig. 2: Contour plots of the (absolute) value of the wave function in the plane of relative coordinates x (horizontal) and y (vertical). The systems have two identical non-interacting particles that both interact with a third particle of the same mass with a zero-range interaction of infinite strength. The upper left panel is the even parity ground state and the upper right is the even parity first excited state, while the lower left panel is the second excited state also for even parity. For comparison, the lower right panel shows the case of two identical fermions and a third particle (of the same mass).

The solutions with odd parity can be obtained in similar fashion by exchanging sine and cosine in $F_i(\phi)$ to obtain

$$\mu \tan\left(\frac{\pi}{3}\mu - \arctan\left(\frac{\tilde{g}_1}{2\mu}\right)\right) - \mu \cot\left(\frac{\pi}{6}\mu\right) - \tilde{g}_2 = 0. \quad (5)$$

In the limit $\tilde{g}_2^{-1} = 0$ and $\tilde{g}_1 = 0$, Eqs. (4) and (5) have two types of solutions; integer for $\mu = 3 + 6n$ with even and $\mu = 6n$ with odd parity, and surprisingly also half-integer for $\mu = 3/2 + 3n$ for odd and even parity. Here $n > 0$ is an integer. If we subsequently let $\tilde{g}_1 \rightarrow \infty$, then only integer solutions remain. The analytical model predicts that this process is smooth, i.e. the half-integer solutions go continuously to integer μ . This implies that non-integer solutions are a generic feature of multi-component bosons. This yields analytical insight to the findings of Ref. [28]. In the absence of a trapping potential, the Bethe ansatz equations for multi-component systems has been discussed [36]. The three-body bound state for $g_1 = 0$ was discussed by Gaudin and Derrida [37]. However, the general case in the limit $g_1 \ll g_2$ is very rarely discussed in the literature.

Numerical solutions. – In order to verify the analytics, we use stochastic variational calculations [38, 39] with $g_1 = 0$ for repulsive $g_2 > 0$. The spectrum is shown in Fig. 1 and confirms the analytical spectrum for $g_2^{-1} \rightarrow 0^+$. Our work therefore demonstrates the applicability of the stochastic variational method to strongly-interacting problems in 1D. The analytical wave functions at $g_2^{-1} = 0$ can be used to calculate the energy to linear order in g_2^{-1} , i.e. $E = E_0 - \frac{K}{g_2}$ (see the appendix for details).

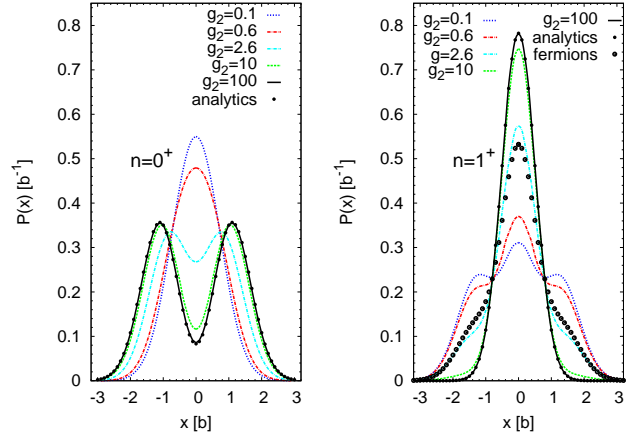


Fig. 3: Density of the single B particle for $g_1 = 0$ for different values of the interparticle interactions in the ground state (left) and first excited state (right) for even parity. Similar results can be obtained for odd parity states. On the right panel we also plot the results for a system where the two identical particles are fermions in the infinite interaction strength limit.

The slope, K , can then be used to show convergence as done in Fig. 1. Note the equal slopes at $g_2^{-1} = 0$ for fractional energy states of both parities. At integer energies, the odd and even solutions never become degenerate (irrespective of g_1) as can be easily checked from Eqs. 4 and 5.

Fractional energy states. – To gain further insight, we show contour plots of the wave functions at $g_2^{-1} = 0$ as functions of the relative coordinates x and y . Panels a, b, and c in Fig. 2 display even parity ground ($E = 2.5\hbar\omega$), first ($E = 4\hbar\omega$), and second excited ($E = 4.5\hbar\omega$) states, respectively. The second excited state has $\mu = 3/2$ and $\nu = 1$, i.e. it contains a radial excitation (visible in Fig. 2 panel c by the node along the vertical axis). Most striking is the presence of regions where the wave functions are zero, and moreover that these regions are complementary for the fractional and integer solutions. This immediately implies that these states are *very* different in spatial structure. The fractional states only allow the three particles to be in configurations where the B coordinate, x_3 , is either larger or smaller than both x_1 and x_2 (so that B is found either on the left or right of *both* A particles). The corresponding density is shown on the left in Fig. 3. For the integer states particle B will always be located between the two A particles, i.e. $x_1 < x_3 < x_2$ or $x_2 < x_3 < x_1$ as shown on the right in Fig. 3. For comparison, we show in Fig. 2 panel d the wave function when the A particles are identical fermions instead [30, 33] and the corresponding density on the right in Fig. 3. The integer energy states with $g_1 = 0$ and $g_2^{-1} = 0$ can be built from spinless fermion wave functions.

The reason for the half-integer energy can be seen from Fig. 2 panel a. The wave function must be symmetric in x by Bose symmetry and vanish when $x_1 = x_3$

and $x_2 = x_3$. The angular part in Eq. (2) must therefore advance its argument by half a period in the 120 degree wedge given by $\pi/6 < \phi < 5\pi/6$ (or equivalently $7\pi/6 < \phi < 11\pi/6$), which means that we have $(2n-1)\pi = 2\pi\mu/3$ or $\mu = 3(2n-1)/2$ with integer $n > 0$. This can be related to classical scattering from wedges in free space [40]. Here a 120 degree wedge (corresponding to our fractional states) is diffractive while a 60 degree wedge (corresponding to our integer states) is not. The diffractionless case implies the existence of a free fermion model and that a Bethe ansatz solution should only be expected in the latter case. Indeed it has been shown recently [41] that $g_1 \neq g_2$ leads to diffractive scattering. We can thus understand our findings as a signature of diffractive and non-diffractive states. In quantum mechanical terms, the distinction can be seen clearly in the three-body wave functions. Due to the factor ρ^μ , it can *only* be expanded in terms of a finite number of single-particle wave functions when μ is integer (and thus mapped to a free fermion model). For non-integer μ this is impossible. This makes the fact that we have a closed formula for a class of the latter type even more interesting.

Order of limits. – An interesting question with a surprising answer concerns the limit where both g_1 and g_2 become large. This can be addressed by using the method introduced in Ref. [34]. The full analytical details can be found in the appendix below. The wave function must now vanish when any two particles overlap, μ goes to an integer ($\mu = 3$ for the lowest state). A physically motivated way to see that the order of limits matters is to consider states like those in Fig. 2 panels a and b which have $g_1 = 0$ and $g_2^{-1} = 0$. Increasing g_1 , the state in panel b is unaffected (no amplitude on the y axis) while the ground state in panel a feels the interaction and goes to $E = 4\hbar\omega$ as $g_1 \rightarrow \infty$. The upper row in Fig. 4 shows the three resulting angular wave functions. In contrast, starting from $g_1^{-1} = 0$ and $g_2 = 0$, the fractional energy state is absent since a node is required along the y -axis. Taking now the limit $g_2 \rightarrow \infty$ produces the wave function in the middle row of Fig. 4. All the cases in the middle row have absolute value of the wave functions and densities identical to the case where the A particles are fermions (shown in Fig. 2d and on the right in Fig. 3) and are thus directly related to the three-body solution for two-component fermions discussed in Ref. [42]. Finally, when $g_1 = g_2 \rightarrow \infty$ we obtain the bottom row in Fig. 4. The far right state which is obtained by using the original Bose-Fermi mapping of Girardeau [3], but two other states emerge. This shows the importance the order of limits in analytical and numerical calculations. Note that all the states in Fig. 4 have energy $E = 4\hbar\omega$, and we thus recover the three-fold degeneracy in the strongly interacting limit [23, 26, 34].

Detection. – The states can be detected by tunneling experiments similar to those used for fermions [10, 43]. For $g_1 = 0$ and g_2 large, we may assume that A and B atoms cannot penetrate each other. Thus only the atom

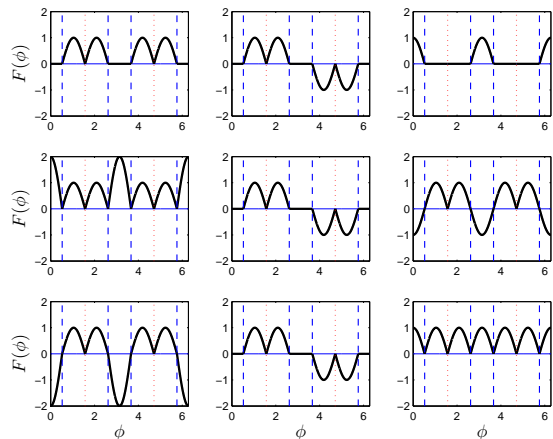


Fig. 4: Angular wave functions, $F(\phi)$, for the entire angular range, $0 \leq \phi \leq 2\pi$, of the exact solutions at $E = 4\hbar\omega$ obtained by taking the limits of diverging g_1 and g_2 in different ways. The three top panels shows the case where $g_2^{-1} = 0$ and then we take $g_1 \rightarrow \infty$, the three middle panels are obtained when $g_1^{-1} = 0$ and then $g_2 \rightarrow \infty$, while the three lower panels are obtained for $g_1 = g_2 \rightarrow \infty$. Vertical dashed (blue) lines are at the overlaps of A and B , while dotted (red) lines are at the overlaps of A and A where Bose symmetry applies. Left and right columns are even parity states, while the middle column has odd parity. Note the orthogonality of the states in each row.

located on the side of the trap where it is opened can tunnel. The fractional state has equal probabilities of spatial AAB and BAA ordering, so 50% of tunnel experiments will produce an AA final state and 50% will produce BA . For integer states, we have ABA structure and always produce an AB final state. Fig. 3 show the two situations and demonstrates that $g_2 \geq 10$ is already close to the fermionized limit. One can also use RF spectroscopy [12] to probe the states by starting from a weakly-interacting AAA system and applying a pulse to drive from internal state A to B in a regime of strong AB interaction. When the driving frequency matches a fractional energy, this should produce the state with an equal probability of AAB and BAA configurations, while if it matches the integer energy we get a pure ABA wave function. The same holds if two atoms are converted from A to B due to the symmetry of the problem. With well-studied Feshbach resonances and previous realizations of a spinor gas we suggest ^{87}Rb for experimental realization [44].

Larger systems. – To show that fractional states appear also for larger systems, we consider three non-interacting A particles and one B . Assume that $g_2^{-1} = 0$ and assume a wave function built from spinless fermions. Since any ordering will always have two adjacent A particles, Bose symmetry implies that we get a cusp when two A particles coincide (absolute value of a spinless fermion wave function). This is not allowed when $g_1 = 0$ and we cannot use spinless fermion wave functions. The argument generalizes to even larger systems. However, structures

like f.x. $ABAB$ and $ABABA$ are still allowed and generally we will have both integer and fraction classes of exact eigenstates. This also applies to Bose-Fermi mixtures. As a means for detecting fractional and integer states for larger systems, we envision a measurement of the momentum distribution which is sensitive to nodes and cusps in the wave function [23]. Since the nodal structure of states like $AAABBB$ and $ABABAB$ are very different we expect distinctly different momentum distributions.

Outlook. – The fractional solutions are unique correlated states with an interesting diffractive classical counterpart. They can provide an excellent benchmark for various numerical procedures and demonstrate the care with which strong interacting limits must be handled. Combined with recent results on 1D fermionic systems [30,34], we now have a full analytical classification of strongly-interacting two-component three-body systems.

This work was supported by the Sapere Aude program starting grant under the Danish Council for Independent Research and by a project grant from the Danish Council for Independent Research - Natural Sciences.

Appendix - Slope of the energy at fermionization. – To obtain the slope of the energy in the different strongly interacting limits, we follow the approach outlined in Ref. [34] and use a linear expansion in $1/g$, where g is the strength of a delta function two-body interaction and we will assume that $g > 0$ here. Writing $E = E_0 - K/g$, we have $K = - \left[\frac{\partial E}{\partial g^{-1}} \right]_{g^{-1}=0}$.

$$K = \lim_{g \rightarrow \infty} g^2 \frac{\sum_{i < j} \int \prod_{i=1}^3 dx_i |\Psi(x_1, x_2, x_3)|^2 \delta(x_i - x_j)}{\langle \Psi | \Psi \rangle}, \quad (6)$$

By using the appropriate boundary condition for a delta-function potential, one can show that g drops out of the calculation of K which depends only on Ψ [34].

First we show how to obtain the slopes shown in Fig. 1 of the main text from the wave functions that we obtain in the analytical model. This is a straightforward matter of inserting those wave functions into the equation for K found in Ref. [34]. Ignoring the center-of-mass part, the wave functions can be written $\Psi(\rho, \phi) = P(\rho)F(\phi)$. The radial parts for the three lowest even parity states shown in Fig. 1 of the main text at $g_1^{-1} = 0$ are $P_0(\rho) = \rho^{3/2} L_0^{3/2}(\rho^2) e^{-\rho^2/2}$, $P_1(\rho) = \rho^3 L_0^3(\rho^2) e^{-\rho^2/2}$ and $P_2(\rho) = \rho^{3/2} L_1^{3/2}(\rho^2) e^{-\rho^2/2}$ where $L_n^m(x)$ is the associated Laguerre polynomial which arises since $U(-n, m+1, x) = (-1)^n n! L_n^m(x)$ for integer n in Eq. (2) of the main text. The angular functions for $\mu = 3/2$ are $\sin(3/2(\phi - \pi/6))$ for $\pi/6 < \phi < 5\pi/6$, $\pm \sin(3/2(\phi - 7\pi/6))$ for $7\pi/6 < \phi < 11\pi/6$ and zero otherwise. The \pm sign is what separates the opposite parity states that become degenerate at $\mu = 3/2$. The excited state with $\mu = 3$ has angular functions $\cos(3\phi)$ for $0 < \phi < \pi/6$ or $11\pi/6 < \phi < 2\pi$, $-\cos(3\phi)$ for $5\pi/6 < \phi < 7\pi/6$ and zero otherwise. Using

these wave functions, we obtain $K_0 = \frac{9}{\sqrt{2\pi^3}}$, $K_1 = \frac{27}{4\sqrt{2\pi}}$ and $K_2 = \frac{117}{20\pi^{3/2}}$. These are the values used to generate the linear fits in Fig. 1. This is not a surprise as the wave functions in the two cases are very different as shown in panel b and panel d of Fig. 2.

Appendix - Limit of strong intra- and inter-component repulsion. – We now address the different ways in which to approach the limit where both g_1 and g_2 go to infinity. This immediately implies that the three-body wave function must be zero whenever any pair of particles overlap. This is only possible using the integer μ solutions. We concentrate on the ground state(s) which have $\mu = 3$. This means that we are in the case where we can use spinless wave functions to express K as a functional of a set of coefficients a_i of the spinless wave function in each region of space of given ordering of the three coordinates x_1 , x_2 , and x_3 . This technique is outlined in Ref. [34] for the case of fermions. The generalization to bosons is a straightforward matter of applying Bose symmetry. Just as in the case of two identical fermions, we may reduce this set of parameters by using parity and Bose symmetry to three. The wave function is then $a_1 \Psi_F$ for $x_2 < x_1 < x_3$ ($\pi/6 < \phi < \pi/2$), $a_2 \Psi_F$ for $x_2 < x_3 < x_1$ ($0 < \phi < \pi/6$ and $11\pi/6 < \phi < 2\pi$), and $a_3 \Psi_F$ for $x_3 < x_1 < x_2$ ($3\pi/2 < \phi < 11\pi/6$). The other orderings are dictated by symmetries. Here the antisymmetrized product state is $\Psi_F \propto \exp(-\frac{\rho^2}{2} - \frac{R^2}{2}) \rho^3 \cos(3\phi)$. The F indicates the common name 'fermionized' state.

We start with the case where we assume that $g_2^{-1} = 0$ and then take the limit $g_1 \rightarrow \infty$. Since $g_2^{-1} = 0$, the interaction term with g_2 is excluded when calculating the slope K from Eq. (6). It implies the boundary condition that the wave function must vanish when non-identical particles coincide. The expression for the slope when $g_1 \rightarrow \infty$ is then determined by the derivatives from points where the two identical bosons overlap. It can be written

$$K = 2\gamma \frac{a_1^2}{a_1^2 + a_2^2 + a_3^2} = 2\gamma \frac{a_1^2}{2a_1^2 + a_2^2}, \quad (7)$$

where in the second equation we use parity and Bose symmetry which implies that $a_1 = a_3$. The factor γ is independent of the a_i coefficients and depends only on the fermionized state Ψ_F . It has the expression

$$\gamma = \frac{\int_{x_1 < x_2} \left| \left[\left(\frac{\partial}{\partial x_2} - \frac{\partial}{\partial x_3} \right)_{x_3 - x_2 \rightarrow 0} \right] \Psi_F \right|^2 dx_1 dx_2}{\int_{x_1 < x_2 < x_3} dx_1 dx_2 dx_3 |\Psi_F|^2}. \quad (8)$$

This factor may be computed using the wave function Ψ_F . Since it is a prefactor it does not influence the relation between the a_i coefficients and we do not calculate it explicitly. As outlined in Ref. [34], one can now obtain the eigenfunctions in the vicinity of $g_1^{-1} = 0$ by finding the extreme points of Eq. (7). By differentiating Eq. (7) with respect to a_1 and a_2 and equating it to zero, one immediately sees that the two solutions are $a_2 = 0$ and a_1 arbitrary or $a_1 = 0$ and a_2 arbitrary. The arbitrary value

is then fixed by normalization. The even parity solution with $a_2 = 0$ is the left panel in the top row of Fig. 4 in the main text, while the one with $a_1 = 0$ is the right panel. The odd parity solution is $a_2 = 0$ and $a_1 = -a_3$ and is shown in the top middle panel in Fig. 4. Note that the solution with $a_1 = 0$ has $K = 0$. This is expected since this solution has energy $E = 4\hbar\omega$ for $g_1 = 0$ and thus its energy does not change as we take $g_1 \rightarrow \infty$. This is clear also from the wave function in panel b of Fig. 2 since this state has zero amplitude in the region where the g_1 interaction is located (along the y -axis).

The second case of interest is the one where we first take $g_1^{-1} = 0$ and then let $g_2 \rightarrow \infty$. Here we exclude the g_1 interaction term when calculating K from Eq. (6) and keep the ones with g_2 . This produces the equation $K = \gamma \frac{(a_1 - a_2)^2}{2a_1^2 + a_2^2}$, where again we have $a_1 = a_3$ as before for positive parity. The extreme points of this equation are $a_1/a_2 = -1/2$ (left panel in the middle row in Fig. 4) and $a_1/a_2 = 1$ (right panel in the middle row in Fig. 4).

Finally, we consider the symmetric case where $g_1 = g_2 \rightarrow \infty$. We retain all three interaction terms when calculating K , and from the point of view of the Hamiltonian all three particles are identical. This gives the expression $K = \gamma \frac{(a_1 - a_2)^2 + 2a_2^2}{2a_1^2 + a_2^2}$, where again we have $a_1 = a_3$ as before for positive parity. The extreme points of this equation are $a_1/a_2 = 1/2$ (left panel in the middle row in Fig. 4) and $a_1/a_2 = -1$ (right panel in the middle row in Fig. 4 in the main text). The change of sign between a_1 and a_2 for the completely symmetric solution occurs because Ψ_F changes sign and this is compensated by $a_1 = -a_2$ to yield the solution that is obtained by Girardeau's Bose-Fermi mapping of the problem [3]. The odd parity state has $a_2 = 0$ (by Bose symmetry) and $a_1 = -a_3$ (combined Bose and parity symmetry). The odd state turns out to be the same irrespective of how the limit is taken.

One can also use the slope to determine the adiabatic connections between strongly interacting and non-interacting states [34]. This requires calculation of γ and insertion of the solutions for a_i in K for the different cases. In the symmetric case where $g_1 = g_2 \rightarrow \infty$, the non-interacting ground state is connected to the Girardeau state in the bottom right panel of Fig. 4. In the two other cases the non-interacting ground state (of even parity) is connected to the wave functions in the left panel of middle and top rows in Fig. 4. This is a clear demonstration of the delicate nature of multi-component bosonic 1D systems with strong short-range interactions.

REFERENCES

[1] I. Bloch, J. Dalibard, and W. Zwerger, *Rev. Mod. Phys.* **80**, 885 (2008).
 [2] L. Tonks, *Phys. Rev.* **50**, 955 (1936).
 [3] M. Girardeau, *J. Math. Phys.* **1**, 516 (1960).
 [4] B. Paredes *et al.*, *Nature (London)* **429**, 277 (2004).

[5] T. Kinoshita, T. Wenger, and D. S. Weiss, *Science* **305**, 1125 (2004).
 [6] T. Kinoshita, T. Wenger, and D. S. Weiss, *Phys. Rev. Lett.* **95**, 190406 (2005).
 [7] E. Haller *et al.*, *Science* **325**, 1224 (2009).
 [8] X. He, P. Xu, J. Wang, and M. Zhan, *Opt. Express* **18**, 13586 (2010).
 [9] F. Serwane *et al.*, *Science* **332**, 336 (2011).
 [10] G. Zürn *et al.*, *Phys. Rev. Lett.* **108**, 075303 (2012).
 [11] R. Bourgain, J. Pellegrino, A. Fuhrmanek, Y. R. P. Sortais, and A. Browaeys, *Phys. Rev. A* **88** 023428 (2013).
 [12] A. N. Wenz *et al.*, *Science* **342**, 457 (2013).
 [13] M. Anderlini *et al.*, *Nature* **448**, 452 (2007).
 [14] S. Fölling *et al.*, *Nature* **448**, 1029 (2007).
 [15] S. Trotzky *et al.*, *Science* **319**, 295 (2008).
 [16] A. Negretti, P. Treutlein, and T. Calarco, *Quantum Inf. Proc.* **10**, 721 (2010).
 [17] J. Simon *et al.*, *Nature* **472**, 307 (2011).
 [18] W. S. Bakr *et al.*, *Nature* **480**, 500 (2011).
 [19] P.-I. Schneider and A. Saenz, *Phys. Rev. A* **85**, 050304(R) (2012).
 [20] H. A. Bethe, *Z. Physik* **71**, 205 (1931).
 [21] M. D. Girardeau and M. Olshanii, *Phys. Rev. A* **70**, 023608 (2004).
 [22] S. Zöllner, H.-D. Meyer, and P. Schmelcher, *Phys. Rev. A* **78**, 013629 (2008).
 [23] F. Deuretzbacher *et al.*, *Phys. Rev. Lett.* **100**, 160405 (2008).
 [24] E. Tempfli, S. Zöllner, and P. Schmelcher, *New J. Phys.* **11**, 073015 (2009).
 [25] M. D. Girardeau, *Phys. Rev. A* **83**, 011601(R) (2011).
 [26] M. D. Girardeau and A. Minguzzi, *Phys. Rev. Lett.* **99**, 230402 (2007).
 [27] M. Valiente, *Europhys. Lett.* **98**, 10010 (2012).
 [28] M. A. Garcia-March *et al.*, *Phys. Rev. A* **88**, 063604 (2013).
 [29] L. Guan, S. Chen, Y. Wang, and Z.-Q. Ma, *Phys. Rev. Lett.* **102**, 160402 (2009).
 [30] E. J. Lindgren *et al.*, *New J. Phys.* **16**, 063003 (2014).
 [31] T. Sowiński, T. Grass, O. Dutta, and M. Lewenstein, *Phys. Rev. A* **88**, 033607 (2013).
 [32] X. Cui and T.-L. Ho, *Phys. Rev. A* **89**, 023611 (2014).
 [33] S. E. Gharashi and D. Blume, *Phys. Rev. Lett.* **111**, 045302 (2013).
 [34] A. G. Volosniev *et al.*, arXiv:1306.4610 (2013).
 [35] N. L. Harshman, *Phys. Rev. A* **86**, 052122 (2012).
 [36] B. Sutherland, *Phys. Rev. Lett.* **20**, 98 (1968).
 [37] M. Gaudin and B. Derrida, *J. Phys. France* **36**, 1183 (1975).
 [38] Y. Suzuki and K. Varga: *Stochastic Variational Approach to Quantum-Mechanical Few-Body Problems*, (Springer-Verlag Berlin Heidelberg, 1998).
 [39] A. G. Volosniev *et al.*, *New J. Phys.* **15**, 043046 (2013).
 [40] F. Oberhettinger, *J. Res. Natl. Bur. Std.* **61**, 343 (1958).
 [41] A. Lamacraft, *Phys. Rev. A* **87**, 012707 (2013).
 [42] L. Guan, S. Chen, Y. Wang, and Z.-Q. Ma, *Phys. Rev. Lett.* **102**, 160402 (2009).
 [43] G. Zürn, A. N. Wenz, S. Murmann, T. Lompe, and S. Jochim, *Phys. Rev. Lett.* **111**, 175302 (2013).
 [44] D. M. Stamper-Kurn and M. Ueda, *Rev. Mod. Phys.* **85**, 1191 (2013).